Research Report

Synthesis of Cu Nanoparticles and Thermal Conductivities of Cu Nanoparticle Joints

Toshitaka Ishizaki, Toshikazu Satoh, Ryota Watanabe, Yasushi Yamada, Fumiaki Osawa, Atsuki Kuno, Atsushi Tane and Masashi Yanase

Report received on Oct. 28, 2013

∎**ABSTRACT**‖   A new synthesis method of Cu nanoparticles capped by fatty acid and amine was studied. In this method, Cu nanoparticles were generated by thermolysis of Cu carbonate at the boiling point of ethylene glycol while preventing nucleations during the temperature rising up to the boiling point, and the reaction finished in short time even with high mol concentration. The capping layers of fatty acid and amine onto the Cu nanoparticles were thermally decomposed just below 300°C under an inert atmosphere which was much lower temperature than that of conventional polymer capping. The thermal conductivities of the Cu nanoparticle joints were measured by the steady heat conduction method. The Cu nanoparticle joint prepared at 350°C exhibited high thermal conductivities of >125 W/mK, which is higher than those of conventional joining materials. The present Cu nanoparticle joint is promising for application in high-output devices used at high temperature because of its high thermal conductivity and melting point.

∎**KEYWORDS**‖   Cu Nanoparticle, Fatty Acid and Amine, Low-temperature Decomposition, Sintering, Joint, Thermal Conductivity, Steady Heat Conduction

1. Introduction

There has been an increasing requirement to improve the output of power semiconductor devices to use the energy source more effectively. Since the output of ordinary Si devices will be difficult to be improved much more in the future, the next-generation devices with compound semiconductors, such as SiC or GaN, have been recently anticipated in practical use to achieve higher output. However, it is an important issue for this application to develop a new joint material which can endure the higher temperature (for example, higher than 200°C) than that in current devices.[1] Pb-rich solder endures the highest temperature among ordinary solders, but there is a movement to inhibit the use of Pb-rich solder because of its toxicity. Therefore, a number of Pb-free materials with relatively high melting points have been studied, such as Au, Zn and Bi-based alloys, but sufficient properties have not been obtained so far.[2-4] A joint material with high melting point and thermal conductivity is demanded to endure the severe operation.

Recently, a new joint technique using low-temperature sintering of nanoparticles has been studied as one of the alternatives to ordinary solders, because surface atoms of nanoparticles are activated so much that they can be sintered at a temperature much lower than the melting point. For example, Ag nanoparticles can be sintered at the same process temperature as ordinary solders and the Ag melting point is 962°C. Ag nanoparticles usually have been used for this purpose since Ag nanoparticles are easily and stably synthesized and have the highest thermal conductivity among metals.[5-10] However, Ag is not appropriate for practical use since it is very expensive and has low resistance against ion migration. On the other hand, Cu nanoparticles are useful since Cu is not only low cost and has high resistance against ion migration, but also its thermal conductivity is almost the same as Ag and its melting point is 1085°C.[11] The Cu nanoparticle joint is strongly anticipated on account of the above mentioned merits.

However, few works about the Cu nanoparticle joint have been reported. The problem is that Cu nanoparticles are aggregated and oxidized more easily than Ag nanoparticles. Therefore, Cu nanoparticles are often produced by using polymers as capping agents, such as poly vinyl pyrrolidone (PVP) and gelatin because the polymer capping is stable.[12-15] However, polymers cannot be decomposed easily, especially under an atmosphere with no oxygen, and so the remaining polymers would inhibit sintering of particles. The previous paper actually reported that capping layers with PVP for Cu nanoparticles were not thermally decomposed even up to 400°C that is too

high for bonding semiconductor chips.[12] Surfactants with low molecular weight are more appropriate for this purpose than polymers, but they are hardly decomposed if their functional groups strongly bond Cu atoms. The previous papers also reported that high joint strength was obtained by Cu nanoparticles capped by cetyl trimethyl ammonium bromide (CTAB) and citric acid, but the process temperature was 400°C.[16,17] To put this technique into practical use, the process temperature should be as low as that of ordinary solders. To overcome this problem, we have studied a new one-pot synthesis of Cu nanoparticles with fatty acid and amine. These nanoparticles can be thermally decomposed at a low temperature even under an inert atmosphere. In this paper, the synthesis method and thermal conductivities of joint samples by the synthesized Cu nanoparticles are reported.

2. Experimental

2. 1 Synthesis

All reagents were used as received without purification. Cu nanoparticles were synthesized using a combination of fatty acid and amine as the capping agent, since this capping agent has been used successfully for synthesizing monodispersed FePt nanoparticles.[18] Cu nanoparticles were synthesized from two types of Cu salts (30 mmol of Cu carbonate ($CuCO_3 \cdot Cu(OH)_2 \cdot H_2O$) or 60 mmol of Cu sulfate ($CuSO_4 \cdot 5H_2O$)) in 300 mL of ethylene glycol ($HO(CH_2)_2OH$) with 30 mmol of oleic acid ($C_{17}H_{33}COOH$) and 30 mmol of oleyl amine ($C_{18}H_{35}NH_2$). Cu sulfate was easily dissolved in ethylene glycol; on the other hand, Cu carbonate was hardly dissolved and mostly sunk to the bottom. The solution in a 500 mL flask was stirred for 30 min at room temperature, then heated to 110°C and kept for 30 min, and finally heated to the boiling point of ethylene glycol and refluxed for 60 min with a nitrogen flow of 0.5 L min^{-1}. The precipitate was washed by solvent, centrifuged at 3000 rpm for 20 min and then dried in a vacuum.

Cu nanoparticles were also synthesized by reducing 120 mmol of Cu carbonate in 600 mL of ethylene glycol with a changing alkyl chain length of 180 mmol of fatty acid and 60 mmol of fatty amine by the same procedure as above. The employed fatty acids and amines were decanoic acid ($C_9H_{19}COOH$) + decyl amine ($C_{10}H_{21}NH_2$), dodecanoic acid ($C_{11}H_{23}COOH$)

+ dodecyl amine ($C_{12}H_{25}NH_2$) and oleic acid + oleyl amine. The synthesized samples are designated as C10, C12 and C18 Cu nanoparticles, respectively, which correspond to the alkyl chain length of fatty acid and amine.

X-ray diffraction (XRD) patterns of the samples were obtained using a RINT-TTR diffractometer (Rigaku) with a CuKα ($\lambda = 0.154$ nm) radiation source. The diffractometer operated at a voltage and a current of 50 kV and 300 mA, respectively.

Transmission electron microscopy (TEM) observations were carried out using a JEM-2000EX instrument (JEOL) with an acceleration voltage of 200 kV for morphological analysis of the samples. Observation samples were prepared by dropping solutions of the Cu nanoparticles onto Cu microgrids with an overlaying amorphous carbon film thickness of about 20 nm. The mean particle size was calculated by arbitrarily measuring 200 particles in a TEM image. For morphological analysis of the large particles, scanning electron microscopy (SEM) observation was also carried out using an S-3600N instrument (Hitachi) with an acceleration voltage of 15 kV.

Ultra violet-visible (UV-Vis) absorption spectra of the samples dispersed in hexane were measured using a UV-2100 spectrometer (Shimadzu) to examine the formation of Cu nanoparticles by the surface plasmon resonance. The samples were obtained by extracting the reaction solutions with hexane.

Thermogravimetric and differential thermal analysis (TG-DTA) was carried out using a TG-DTA instrument (Rigaku) to examine the thermal decomposition behaviors of the capping layers. This analysis was performed with an argon gas flow of 100 mL min^{-1}, because the weight ratio of the sample increased significantly in air due to oxidation, thereby making it difficult to measure the decomposition temperature of the capping layers accurately. The temperature was increased from RT to 500°C at a rate of 20°C min^{-1}. The amount of capping layers was estimated from the total loss of weight ratio.

2. 2 Evaluation of Thermal Conductivity

In this study, thermal conductivities were evaluated by the steady heat conduction method of a joint sample because it is known that an ordinary method for thermal conductivity, such as the laser flash method, cannot evaluate it precisely in the case of a thin film. The cross-sectional view and dimensions of the joint

sample are shown in **Fig. 1** and **Table 1**, respectively. Cu nanoparticle paste, which was prepared by mixing decanol and α-terpineol with the Cu nanoparticle powder, was used to join the ceramic heater chip with a Ni surface onto the baseplate with a Ni surface. The Cu nanoparticle paste was printed onto the center of the baseplate by using a metal mask with an area of 6×6 mm^2 and a thickness of 0.15 mm. The heater chip was placed onto the printed Cu nanoparticle paste. The heater chips and the baseplates were joined in a hydrogen atmosphere with a pressure of 1 MPa for 5 min at 250 or 350°C. The joint samples are designated as C10, C12 and C18 Cu nanoparticle joints, corresponding to the alkyl chain length of fatty acid and amine of the Cu nanoparticle, respectively. The joint sample was fixed on the heatsink by the thermal grease.

The thermal flux of 100 W/cm^2 was applied to the heater chip and the temperature of the heatsink was controlled to be constant by cooling water of 65°C from a circulation unit. The water flow rate was 3 L min^{-1}. The thermal resistance (R_{th}) was estimated by the following equation:

$$R_{th} = (T_{on}-T_{off})/P$$

where T_{on} and T_{off} are the temperatures of power on and off, respectively, and P is the input electrical power to the heater chip.

Thermal conductivity estimations were carried out by the three-dimensional finite element method. Because it was difficult to analytically determine a thermal transfer coefficient of the active heatsink to cooling water, it was estimated from the measured whole thermal resistance of the sample joined by conventional solder (Sn-0.7Cu). The thermal transfer coefficient was estimated to be 9000 W/m^{2}K. The thermal conductivities of the Cu nanoparticle joints were estimated from the thermal resistances with the pre-determined thermal transfer coefficient from the soldered sample and the measured thicknesses of the joint layer. The thicknesses of the joint layers were 0.1, 0.2 and 0.4 mm by the C10, C12 and C18 Cu nanoparticles, respectively.

3. Results and Discussion

3. 1 Synthesis of Cu Nanoparticles

Figure 2(a) shows XRD patterns of the synthesized samples from (I) Cu sulfate and (II) Cu carbonate. The
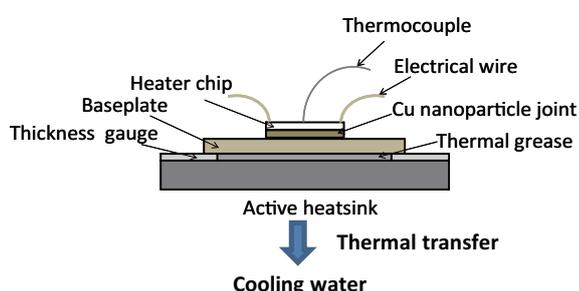
Fig. 1   Schematic view of the Cu nanoparticle joint sample for estimating its thermal conductivity.

Table 1   Dimensions and thermal conductivities of materials of the Cu nanoparticle joint sample (t* = 0.1 to 0.4)

Component	Material	Dimension (mm)	Conductivity (W/mK)
Heater chip	Al$_2$O$_3$	$6 \times 6 \times 0.5$	20
Cu NP joint	Cu	$6 \times 6 \times$ t*	**_Estimate_**
Baseplate	Cu-65Mo	$20 \times 40 \times 3$	207
Thermal grease	Silicone	$20 \times 40 \times 0.06$	4.5
Active heatsink	Al	$85 \times 194 \times 5$	140
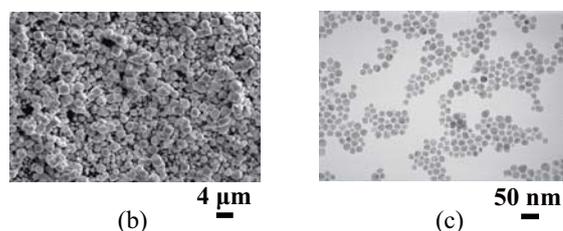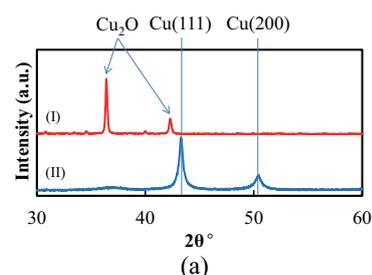
Fig. 2   (a) XRD patterns of the samples synthesized from (I) Cu sulfate and (II) Cu carbonate using oleic acid and oleyl amine as the capping agent. (b) SEM micrograph of the Cu$_2$O particles synthesized from Cu sulfate. (c) TEM micrograph of the Cu nanoparticles synthesized from Cu carbonate.

sample from Cu sulfate exhibits diffraction peaks which agree with those in the spectrum of Cu_2O particles shown in the previous paper.[19] The SEM micrograph of the sample from Cu sulfate exhibits cubic and angular particles with diameters of more than 1 μm, as shown in Fig. 2(b). On other hand, the sample from Cu carbonate exhibits diffraction peaks mainly from Cu, as shown in the XRD pattern of Fig. 2(a) and spherical particles with diameters of about 20 nm, as shown in the TEM micrograph of Fig. 2(c). Therefore, it is revealed that Cu nanoparticles can be synthesized from Cu carbonate by this method even though Cu carbonate cannot be dissolved in ethylene glycol.

Figure 3 shows photos of the samples extracted from the reaction solutions at (a) 180°C and (b) 190°C, (c) refluxing for 0 min and (d) refluxing for 3 min during synthesis of Cu nanoparticles from Cu carbonate, and (e) their UV-vis absorption spectra. The sample color changes from blue to red as the reaction temperature increases. A peak appears around 575 nm at refluxing for 0 min and it becomes clear after 3 min. This characteristic peak is well known as the surface plasmon resonance of the Cu nanoparticle reported in previous papers.[20-22] The red color of this solution is attributed to this absorption peak.

The UV-Vis absorption spectra indicate that Cu nanoparticles are formed immediately after the solution is heated up to the boiling point during this reaction. The typical synthesis for nanoparticles is carried out by reducing metal ions with metal salts dissolved in solution, but it has the problem that particles tend to grow by aggregation of the initial formed nuclei during the solution temperature increases if metal ions can be reduced at low temperature. In our method, insoluble Cu salt cannot be decomposed until the boiling point and initial nucleations do not occur during the solution temperature increases. Insoluble Cu salt is suddenly decomposed at the boiling point of ethylene glycol and reduced to generate nuclei homogeneously. The particle size is maintained to be small by connecting with the capping agent of oleic acid and amine. This reaction is completed in a short time even with a high mol concentration of Cu. Therefore, this method suggests an advantage that enables mass production of Cu nanoparticles.[23]

Figure 4(a) shows XRD patterns of the synthesized samples changing the alkyl chain length of fatty acid

(a) 180 °C   (b) 190 °C   (c) Reflux 0min   (d) Reflux 3min

(e)

Fig. 3 Photos of the samples dispersed hexane extracted from the reaction solution at (a) 180°C, (b) 190°C, (c) refluxing for 0 min, and (d) for 3 min during synthesis of the Cu nanoparticles from Cu carbonate using oleic acid and oleyl amine as capping agents and (e) their UV-Vis absorption spectra.

(a)

(b) C10   (c) C12
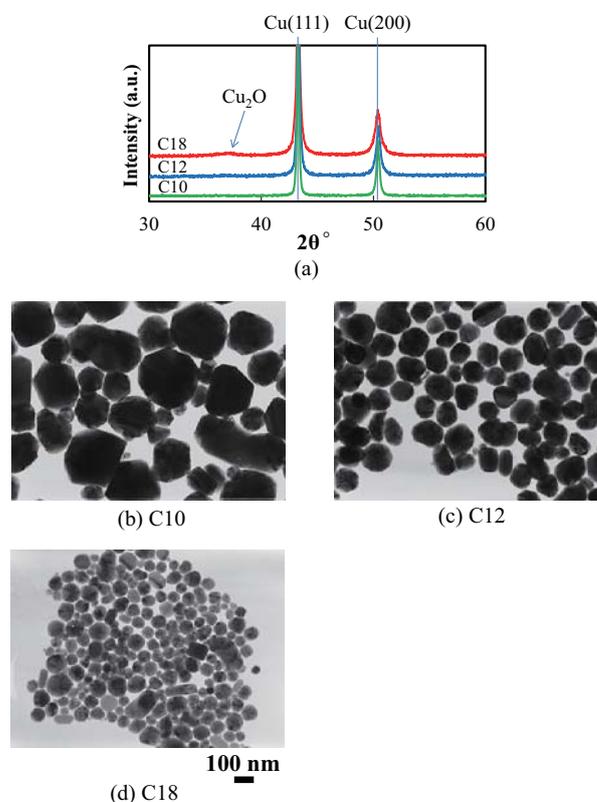
(d) C18

Fig. 4 (a) XRD patterns and (b)-(d) TEM micrographs of the C10, C12 and C18 Cu nanoparticles.

and amine from C10 to C18. All the samples mainly exhibit diffraction peaks from Cu, but the C18 Cu nanoparticles exhibit a weak peak from Cu_2O in addition to the Cu peak. TEM micrographs of the Cu nanoparticles exhibit mean particle sizes that are approximately 231 ± 77.9, 135 ± 29.0 and 64.8 ± 19.0 nm for the C10, C12 and C18 Cu nanoparticles, respectively, as shown in Figs. 4(b) - (d). This result suggests that the particle size is decreased due to enhancement of steric hindrance as the alkyl chain length of fatty acid and amine increases. When Cu nanoparticles are too small, the nano-scale Cu surface would be unstable in the air so that oxidation could not be prevented even with the capping layers. Therefore, the C18 Cu nanoparticles are slightly oxidized, as shown in the XRD pattern.

The thermal decomposition behaviors of the capping layers were examined by TG-DTA analyses, as shown in **Figs. 5**(a) - (c). The C10, C12 and C18 Cu

nanoparticles exhibit exothermic peaks at 288, 292 and 300°C, respectively. These peaks indicate that the thermal decomposition temperature of the capping layer with fatty acid and amine is just below 300°C even under an inert atmosphere which is much lower in temperature than that of the PVP capping.[12] The amount of capping layers on the C10, C12 and C18 Cu nanoparticles are 0.74, 1.23 and 2.86%, respectively. It is assumed that the ratio of capping layers to total mass increases as the alkyl chain length increases because the particle size decreases and the molecular mass of fatty acid and amine increases.

3. 2 Thermal Conductivity of the Cu Nanoparticle Joint

Figure 6 shows thermal resistances of the Cu nanoparticle joints. The thermal resistances by joining at 350°C are lower than those by joining at 250°C in all cases because the capping layers cannot be decomposed at 250°C and so sintering of the Cu nanoparticles is inhibited by residues. On the other hand, the Cu nanoparticles can be sintered at 350°C more densely due to complete decomposition of the capping layers, and this results in decreasing thermal resistances compared with those joined at 250°C.

Figure 7 shows thermal conductivities of the Cu nanoparticle joints estimated from their thermal resistances. The C10 Cu nanoparticle joint prepared at 250°C has the lowest thermal conductivity because the C10 Cu nanoparticles are too large to be sufficiently sintered compared with the C12 and C18 Cu nanoparticles at this temperature. On the other hand, the C12 Cu nanoparticle joint exhibits higher thermal conductivity than that of the C18 Cu nanoparticle joint

Fig. 5 (a) - (c) TG-DTA results of the C10, C12 and C18 Cu nanoparticles.
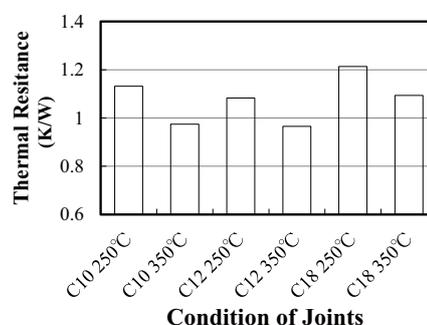
Fig. 6 Measured thermal resistances of the C10, C12 and C18 Cu nanoparticle joints at 250 and 350°C.

prepared at 250°C. It is assumed that the oxidized layers could prevent the C18 Cu nanoparticles from sintering so that its thermal conductivity would be smaller than that of the C12 Cu nanoparticle joint.

The thermal conductivities by joining at 350°C are higher than those by joining at 250°C in all cases because the Cu nanoparticles could be sintered due to complete decomposition of the capping layers at this temperature. The thermal resistances of the C10 and C12 Cu nanoparticle joints prepared at 350°C are small enough that their thermal conductivities cannot be calculated precisely by our method. Their thermal conductivities are approximately determined to be higher than 125 W/mK in this study. On the other hand, the thermal conductivity of the C18 Cu nanoparticle joint prepared at 350°C is almost 125 W/mK, which is lower than those of the C10 and C12 Cu nanoparticle joints. It is assumed that the oxidized surfaces would inhibit sintering in the case of the C18 Cu nanoparticles so that the thermal conductivity would be lower.

Table 2 shows a comparison of melting points and thermal conductivities between the Cu nanoparticle joint and the candidate joining materials used for higher temperature conditions than those in the ordinary devices referred to in previous papers.[3,24,25] Since Cu_3Sn and Cu_6Sn_5 are the main compounds of Cu-Sn transient liquid phase (TLP) soldering, their properties are added to the list.[26] It is noteworthy that the Cu nanoparticle joint has the highest melting point and thermal conductivity compared with other materials. Therefore, it can be concluded that the Cu nanoparticle joint shows the best property for the next-generation device.

Table 2 Comparison of melting points and thermal conductivities between the Cu nanoparticle joint and conventional joining materials used for higher temperature condition than ordinary devices.

Material	Melting Point (ºC)	Thermal Conductivity (W/mK)
Cu nanoparticle	**1085**	**>125**
Zn-5Al	380	117
Cu_3Sn	640	70
Cu_6Sn_5	415	34
Pb-5Sn	314	36
Au-20Sn	280	59
Bi+CuAlMn	270	8

Zn-5Al, Bi+CuAlMn: Ref. 3
Cu_3Sn, Cu_6Sn_5: Ref. 24
Pb-5Sn, Au-20Sn: Ref. 25

4. Conclusion

Cu nanoparticles capped by fatty acid and amine were successfully synthesized by thermolysis of Cu carbonate in ethylene glycol. The capping layer was thermally decomposed in an inert atmosphere below 300°C, which is much lower than those of conventional PVP capping. The Cu nanoparticle joint prepared at 350°C exhibited high thermal conductivity (>125 W/mK), which is higher than those of conventional joining materials. The present Cu nanoparticle joint is promising for application in high-output devices used at high temperatures due to the high thermal conductivities and the high melting point.

Fig. 7 Calculated thermal conductivities of the C10, C12 and C18 Cu nanoparticle joints at 250 and 350 °C.

References

(1) Chin, H. S., Cheong, K. Y. and Ismail, A. B., "A Review on Die Attach Materials for SiC-based High-temperature Power Devices", *Metall. Mater. Trans. B*, Vol. 41B (2010), pp. 824-832.

(2) Kim, S., Kim, K.-S., Suganuma, K. and Izuta, G., "Interfacial Reactions of Si Die Attachment with Zn-Sn and Au-20Sn High Temperature Lead-free Solders on Cu Substrates", *J. Electron. Mater.*, Vol. 38, No. 6 (2009), pp. 873-883.

(3) Yamada, Y., Takaku, Y., Yagi, Y., Nakagawa, I., Atsumi, T., Shirai, M., Ohnuma, I. and Ishida, K., "Pb-free High Temperature Solder Joints for Power Semiconductor Devices", *Trans. Jpn. Inst. Electron. Packag.*, Vol. 2, No. 1 (2009), pp. 79-84.

(4) Yamada, Y., Takaku, Y., Yagi, Y., Nakagawa, I., Atsumi, T., Shirai, M., Ohnuma, I. and Ishida, K., "Reliability of Wire-bonding and Solder Joint for High Temperature Operation of Power Semiconductor Device", *Microelectron. Reliab.*, Vol. 47 (2007), pp. 2147-2151.

(5) Siow, K. S., "Mechanical Properties of Nano-silver Joints as Die Attach Materials", *J. Alloys. Compd.*, Vol. 514 (2012), pp. 6-19.

(6) Ide, E., Angata, S., Hirose, A. and Kobayashi, K. F., "Metal-metal Bonding Process Using Ag Metallo-organic Nanoparticles", *Acta. Mater.*, Vol. 53 (2005), pp. 2385-2393.

(7) Quintero, P. O. and McCluskey, F. P., "Temperature Cycling Reliability of High-temperature Lead-free Die-attach Technologies", *IEEE Trans. Dev. Mater. Reliab.*, Vol. 11, No. 4 (2011), pp. 531-539.

(8) Hu, A., Guo, J. Y., Alarifi, H., Patane, G., Zhou, Y., Compagniti, G. and Xu, C. X., "Low Temperature Sintering of Ag Nanoparticles for Flexible Electronics Packaging", *Appl. Phys. Lett.*, Vol. 97 (2010), 153117.

(9) Morita, T., Ide, E., Yasuda, Y., Hirose, A. and Kobayashi, K., "Study of Bonding Technology Using Silver Nanoparticle", *Jpn. J. Appl. Phys.*, Vol. 47 (2008), pp. 6615-6622.

(10) Lei, T. G., Calata, J. N., Lu, G. Q., Xu, C. and Luo, S., "Low-temperature Sintering of Nanoscale Silver Paste for Attaching Large-area (> 100 mm^2) Chips", *IEEE Trans. Comp. Packag. Technol.*, Vol. 33, No. 1 (2010), pp. 98-104.

(11) Morisada, Y., Nagaoka, T., Fukusumi, M., Kashiwagi, Y., Yamamoto, M. and Nakamoto, M., "A Low-temperature Bonding Process Using Mixed Cu-Ag Nanoparticles", *J. Electron. Mater.*, Vol. 39, No. 8 (2010), pp. 1283-1288.

(12) Yan, J., Zou, G., Hu, A. and Zhou, Y. N., "Preparation of PVP Coated Cu NPs and the Application for Low-temperature Bonding", *J. Mater. Chem.*, Vol. 21 (2011), pp. 15981-15986.

(13) Jeong, S., Woo, K., Kim, D., Lim, S., Kim, J. S., Shin, H., Xia, Y. and Moon, J., "Controlling the Thickness of the Surface Oxide Layer on Cu Nanoparticles for the Fabrication of Conductive Structures by Ink-jet Printing", *Adv. Funct. Mater.*, Vol. 18 (2008), pp. 679-686.

(14) Choi, C. S., Jo, Y. H., Kim, M. G. and Lee, H. M., "Control of Chemical Kinetics for Sub-10 nm Cu Nanoparticles to Fabricate Highly Conductive Ink Below 150°C", *Nanotechnology*, Vol. 23 (2012), 065601.

(15) Yonezawa, T., Takeoka, S., Kishi, H., Ida, K. and Tomonari, M., "The Preparation of Copper Fine Particle Paste and Its Application as the Inner Electrode Material of a Multilayered Ceramic Capacitor", *Nanotechnology*, Vol. 19 (2008), 145706.

(16) Kobayashi, Y., Shirochi, T., Yasuda, Y. and Morita, T., "Preparation of Metallic Copper Nanoparticles in Aqueous Solution and Their Bonding Properties", *Solid State Sci.*, Vol. 13 (2011), pp. 553-558.

(17) Kobayashi, Y., Shirochi, T., Yasuda, Y. and Morita, T., "Metal-metal Bonding Process Using Metallic Copper Nanoparticles Prepared in Aqueous Solution", *Int. J. Adh. Adh.*, Vol. 33 (2012), pp. 50-55.

(18) Sun, S., Murray, C. B., Weller, D., Folks, L. and Moser, A., "Monodisperse FePt Nanoparticles and Ferromagnetic FePt Nanocrystal Superlattices", *Science*, Vol. 287 (2000), pp. 1989-1992.

(19) Long, J., Dong, J., Wang, X., Ding, Z., Zhang, Z., Wu, L., Li, Z. and Fu, X., "Photochemical Synthesis of Submicron- and Nano-scale Cu$_2$O Particles", *J. Colloid Interface Sci.*, Vol. 333 (2009), pp. 791-799.

(20) Abdulla-Al-Mamun, M., Kusumoto, Y. and Muruganandham, M., "Simple New Synthesis of Copper Nanoparticle in Water/Acetonitrile Mixed Solvent and Their Characterization", *Mater. Lett.*, Vol. 63 (2009), pp. 2007-2009.

(21) Bicer, M. and Sisman, I., "Controlled Synthesis of Copper Nano/Microstructures Using Ascorbic Acid in Aqueous CTAB Solution", *Powder Tech.*, Vol. 198 (2010), pp. 279-284.

(22) Korchev, A. S., Shulyak, T. S., Slaten, B. L., Gale, W. F. and Mills, G., "Sulfonated Poly(Ether Ether Ketone)/Poly(Vinyl Alcohol) Sensitizing System for Solution Photogeneration of Small Ag, Au, and Cu Crystallites", *J. Phys. Chem. B*, Vol. 109 (2005), pp. 7733-7745.

(23) Wu, S.-H., and Chen, D.-H., "Synthesis of High-concentration Cu Nanoparticles in Aqueous CTAB Solutions", *J. Colloid Interf. Sci.*, Vol. 273 (2004), pp. 165-169.

(24) Yao, Y., Fry, J., Fine, M. E. and Keer, L. M., "The Wiedemann-Franz-Lorenz Relation for Lead-free Solder and Intermetallic Materials", *Acta Mater.*, Vol. 61 (2013), pp. 1525-1536.

(25) Kim, S., Kim, K.-S., Kim, S.-S. and Suganuma, K., "Interfacial Reaction and Die Attach Properties of Zn-Sn High-temperature Solders", *J. Electron. Mater.*, Vol. 38, No. 2 (2009), pp. 266-272.

(26) Li, J. F., Agyakwa, P. A. and Johnson, C. M., "Interfacial Reaction in Cu/Sn/Cu System During the Transient Liquid Phase Soldering Process", *Acta Mater.*, Vol. 59 (2011), pp. 1198-1211.

Yamada, Y., "Thermal Characterizations of Cu Nanoparticle Joints for Power Semiconductor Devices", © 2013 Elsevier.

Figs. 2 and 3
Adapted from J. Mater. Chem., Vol. 22 (2012), pp. 25198-25206, Ishizaki, T. and Watanabe, R., "A New One-pot Method for the Synthesis of Cu Nanoparticles for Low Temperature Bonding", © 2012 The Royal Society of Chemistry, with permission from the Royal Society of Chemistry.

Toshitaka Ishizaki
  Research Fields:
    - Metallic Nanoparticle
    - Joint Technology
    - Sintering
  Academic Degree: Dr.Eng.
  Academic Societies:
    - The Japan Institute of Metals and Materials
    - The Chemical Society of Japan
    - The Society of Nano Science and Technology
    - American Chemical Society

Toshikazu Satoh
  Research Fields:
    - Joints in Electronics Packaging
    - Interface Analysis
  Academic Societies:
    - The Japan Society of Applied Physics
    - The Japan Institute of Electronics Packaging
    - OLED Forum Japan

Ryota Watanabe
  Research Fields:
    - Metallic Nanoparticle
    - Joint Technology
    - Sintering
  Academic Degree: Dr.Eng.
  Academic Society:
    - Catalysis Society of Japan

Yasushi Yamada*
  Research Fields:
    - Electronic Packaging
    - Electronic Material
    - Chemical Sensor
    - Electronic Circuit
  Academic Degree: Dr.Eng.
  Academic Societies:
    - The Institute of Electrical Engineers of Japan
    - The Japan Institute of Electronics Packaging

Fumiaki Osawa*
  Research Fields:
    - Integrated Sensors and Intelligence
    - Robotics
    - Motion Control
  Academic Degree: Dr.Eng.
  Academic Societies:
    - The Institute of Electrical Engineers of Japan
    - The Japan Society for Precision Engineering

Atsuki Kuno*
  Research Fields:
    - Electronic Packaging
    - Electronic Circuit Simulation
  Academic Societies:
    - The Institute of Electrical Engineers of Japan
    - The Japan Institute of Electronics Packaging

Atsushi Tane*
  Research Fields:
    - Chemical Sensor
    - Electronic Packaging
  Academic Society:
    - Society of Automotive Engineers of Japan
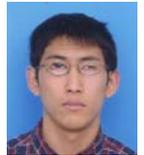
Masashi Yanase*
  Research Field:
    - Electronic Packaging
  Academic Society:
    - The Japan Institute of Electronics Packaging

*Daido University